

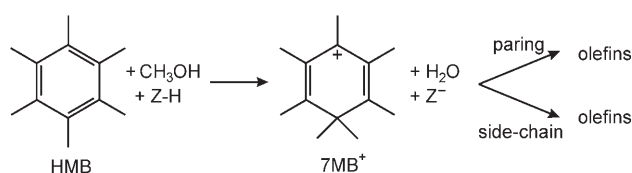
# Zeolite Shape-Selectivity in the *gem*-Methylation of Aromatic Hydrocarbons\*\*

David Lesthaeghe,\* Bart De Sterck, Veronique Van Speybroeck, Guy B. Marin, and Michel Waroquier\*

Herein, we explicitly demonstrate the importance of transition-state-shape selectivity for the conversion of methanol to light olefins (methanol-to-olefins or MTO). The MTO process in acidic zeolites is a prominent research topic, driven both by the possibility of monetizing stranded natural gas reserves, coal, or even biomass and by the ever-increasing demands for ethene derivatives.<sup>[1]</sup> For the last 30 years, the actual reaction mechanism of this process has been a topic of considerable debate, fueled by countless and often conflicting propositions.<sup>[1,2]</sup> Most efforts centered on mechanisms proposing “direct” formation of ethene from only methanol and C<sub>1</sub> derivatives. Recently, however, experimental studies by Haw and co-workers<sup>[3,4]</sup> as well as our own theoretical results<sup>[5]</sup> provided strong evidence for the complete failure of the direct routes.

The most likely alternative, which is more in accordance with experimental observations,<sup>[6]</sup> is given by the “hydrocarbon-pool” (HP) proposal,<sup>[7,8]</sup> in which organic species trapped in the zeolite pores undergo repeated methylation followed by olefin elimination. To date, the elementary steps governing this process are not well understood. Ideally, experimental and theoretical efforts should complement each other in unraveling this complex network of reactions. A hydrocarbon pool consisting mainly of polymethylbenzenes has been shown to be active for olefin formation,<sup>[9,10]</sup> independent of the zeotype catalyst chosen.<sup>[11]</sup> Additionally, there is strong experimental evidence for cyclic resonance-stabilized cations as persistent species in the pores, such as cyclopentenyl and pentamethylbenzenium cations in HZSM-5<sup>[12,13]</sup> and hexamethylbenzenium and heptamethylbenzenium (7MB<sup>+</sup>) cations in HBEA.<sup>[14,15]</sup> Geminal methylbenzenium ions form the main starting point from which commonly

proposed HP routes (such as the “paring” and “side-chain” mechanisms) originate.<sup>[16]</sup> The heptamethylbenzenium cation, for example, is formed from hexamethylbenzene (HMB) through one-step geminal methylation by methanol as shown in Scheme 1.



**Scheme 1.** Initiating step for the formation of olefins from hexamethylbenzene (HMB). Z = zeolite.

The product distribution is defined by the number of methyl groups on the active hydrocarbon-pool species: propene is favored by methylbenzenes with four to six methyl groups, while ethene is predominantly formed from the lower methylbenzenes.<sup>[17]</sup> As the hydrocarbon-pool mechanism involves bulky cyclic intermediates, it is also a space-demanding process. Therefore, zeolite topology is crucial in defining the hydrocarbon pool, resulting in a strong topological dependence of product distribution as well. The active catalyst is a combined organic–inorganic supramolecular complex of the zeolite framework and the hydrocarbon pool.<sup>[2]</sup>

Just recently, Cui et al. have reported experimental evidence for transition-state-shape selectivity in studies of methanol-to-olefin conversion on zeolites with varying pore size.<sup>[18]</sup> Experimental claims to transition-state-shape selectivity are, ideally, verified by theoretical methods,<sup>[19–21]</sup> since these are more suited for elucidating the extent to which the local shape of the pore influences local reaction rates. To the best of our knowledge, ours is the first theoretical study on the hydrocarbon-pool proposal to take topological concepts explicitly into account, by focusing on both the electrostatic stabilization and geometrical constraints of typical zeolite frameworks on key carbenium ions and transition states.

To separate the effects of hydrocarbon-pool species and zeolite topology, the geminal methylation of several methylbenzenes, ranging from toluene, over *p*-xylene, 1,2,4-trimethylbenzene (pseudocumene), 1,2,4,5-tetramethylbenzene (durene), and pentamethylbenzene (PMB) to hexamethylbenzene (HMB), was first modeled on 5T clusters. These small clusters represent any aluminosilicate and neglect all framework steric and electrostatic effects. Figure 1a shows the energy barriers and reaction energies for the methylation

[\*] Ir. D. Lesthaeghe, Ir. B. De Sterck, Dr. Ir. V. Van Speybroeck, Prof. Dr. M. Waroquier  
 Center for Molecular Modeling  
 Ghent University  
 Proeftuinstraat 86, 9000 Gent (Belgium)  
 Fax: (+32) 9-264-6697  
 E-mail: david.lesthaeghe@ugent.be  
 michel.waroquier@ugent.be  
 Homepage: <http://molmod.ugent.be>  
 Prof. Dr. Ir. G. B. Marin  
 Laboratorium voor Petrochemische Techniek  
 Ghent University  
 Krijgslaan 281-S5, 9000 Gent (Belgium)

[\*\*] This work is supported by the Fund for Scientific Research—Flanders (FWO) and the Research Board of Ghent University.

Supporting information for this article is available on the WWW under <http://www.angewandte.org> or from the author.

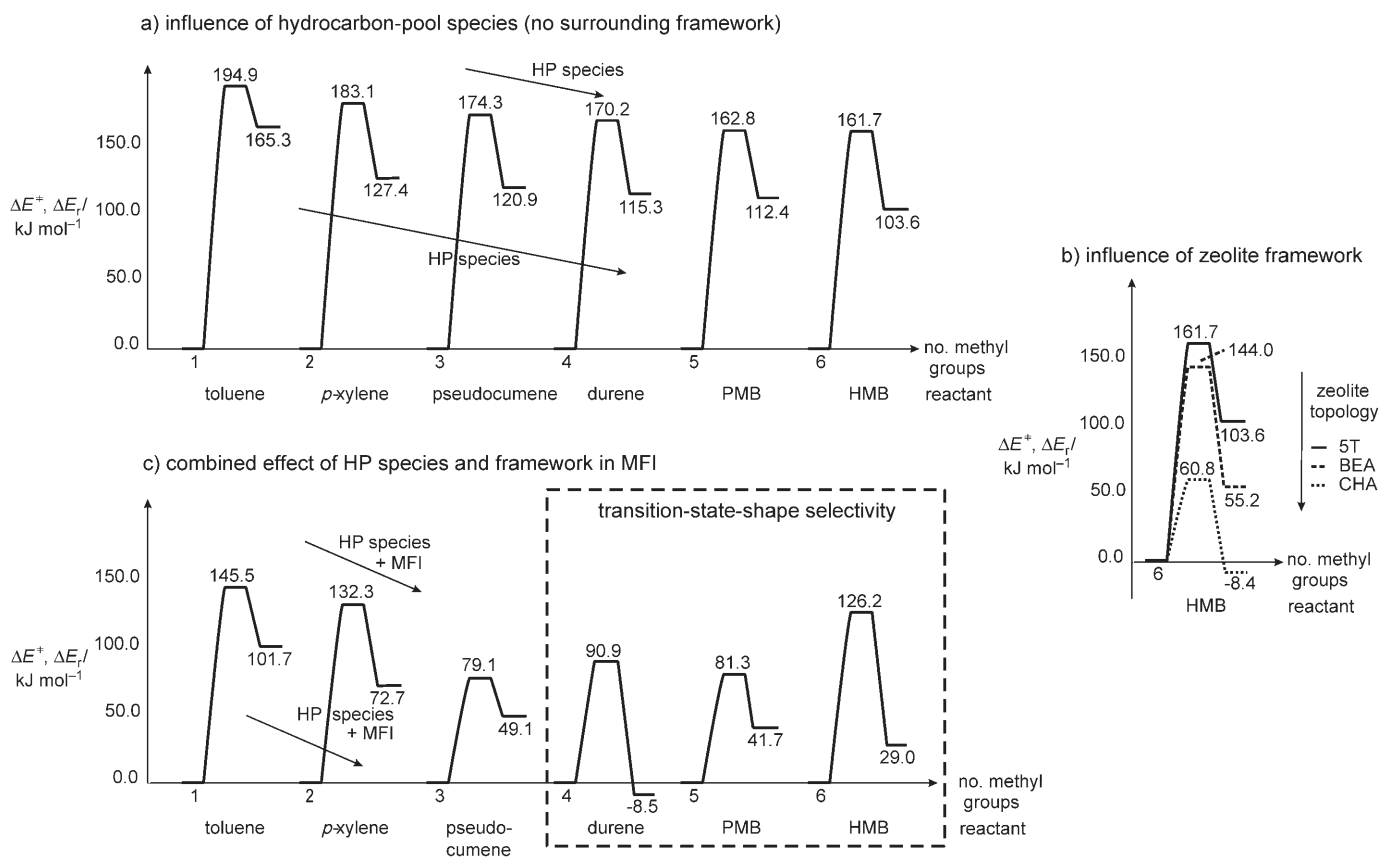


**Figure 1.** Barrier heights  $\Delta E^\ddagger$  and reaction energies  $\Delta E_r$  in  $\text{kJ mol}^{-1}$  for a) geminal methylation of different polymethylbenzenes in the 5T cluster, b) geminal methylation of hexamethylbenzene in the zeolite topologies BEA and CHA, and c) geminal methylation of different polymethylbenzenes in the space-limiting MFI structure.

of a series of polymethylbenzenes in the 5T cluster. A steady decrease in both the reaction barrier  $\Delta E^\ddagger$  (from 194.9 to 161.7  $\text{kJ mol}^{-1}$ ) and the reaction energy  $\Delta E_r$  (from 165.3 to 103.6  $\text{kJ mol}^{-1}$ ) is observed with the increasing number of methyl groups. Our results for HMB in 5T are similar to the values calculated earlier for HMB in 4T (169  $\text{kJ mol}^{-1}$  and 108  $\text{kJ mol}^{-1}$ ).<sup>[22]</sup> While these results clearly illustrate the increase of reactivity for higher polymethylbenzenes, the barriers remain relatively high in absolute value. It is expected that the zeolite framework lends additional electrostatic stabilization to the ion pair formed by the cation and the negative aluminum defect.<sup>[23]</sup> Therefore, the calculations were extended to more advanced 44T and 46T clusters, which represent both the active site and the surrounding zeolite cage<sup>[23,24]</sup> for various industrially and academically important topologies, such as BEA, CHA, and MFI (shown in Figure 2).

The beta zeolite (BEA topology) has a large pore structure that allows direct introduction of large molecules such as hexamethylbenzene. It is an interesting topology for mechanistic studies, although it is not used as a commercial catalyst because of rapid coke formation and deactivation. Calculations with the BEA topology (Figure 1b) shows an only slightly reduced reaction barrier of 144.0  $\text{kJ mol}^{-1}$  and a reaction energy of 55.2  $\text{kJ mol}^{-1}$ . As shown in Figure 2, the large cages in BEA provide limited electrostatic interaction with the organic species that are located centrally in the pores.

Modeling the aluminosilicate chabazite (CHA topology) is a first step towards the commercially important aluminophosphate HSAPO-34, which has the same topology as CHA but an entirely different composition. Composition effects should, however, be treated separately from pure topology effects, and these will be part of a future study. The CHA topology is a structure with spacious cages interconnected by small windows. Methylbenzenes are formed through a “ship-in-a-bottle” synthesis and remain trapped in the catalyst.<sup>[9]</sup> The calculations with the CHA topology (Figure 1b) shows a spectacular reduction in energetics. The reaction barrier of merely 60.8  $\text{kJ mol}^{-1}$  is easily surmountable, and the reaction energy of  $-8.4 \text{ kJ mol}^{-1}$  even hints at an exothermic initiation of the hydrocarbon-pool cycle in chabazite. Apparently, the enclosing chabazite topology provides an ideal setting for this key reaction step. The term “inverse shape selectivity” immediately springs to mind, although this terminology is usually reserved for the preferential adsorption of neutral branched paraffins rather than for charged species.<sup>[25,26]</sup> Direct comparison between BEA and CHA clearly shows the strong difference between open and dense framework topologies in solvating this crucial intermediate.

Even though they differ greatly in cage dimensions, both beta and chabazite zeolites contain sufficiently large cages not to impose any geometric constraints on the transition state. This is not the case for HZSM-5, an industrially important

zeolite exhibiting the medium-pore MFI topology containing two sets of intersecting channels. Durene is the largest polymethylbenzene that can be introduced directly along the narrow channels.<sup>[27]</sup> Although MFI does not boast spacious cages, HMB could be formed in the extended space available at the channel intersections. However, its diffusion and reactivity will be sterically restricted. This limited space imposes severe problems for the geminal methylation of methylbenzenes. The spatial demand of the transition state in particular is shown in Figure 2: the two-dimensional methyl-

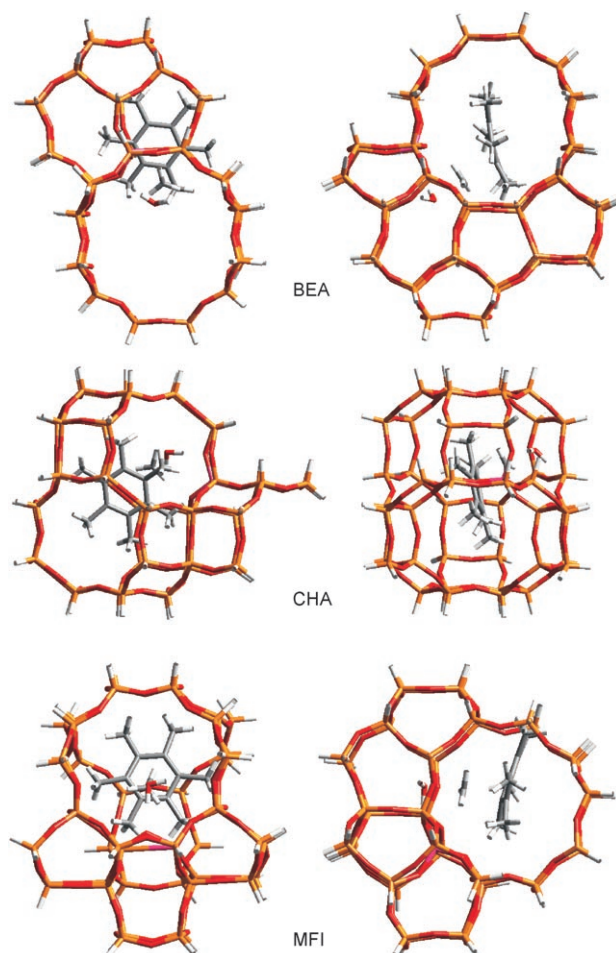


**Figure 2.** Transition-state geometries for the formation of heptamethylbenzenium in the BEA, CHA, and MFI zeolite topologies.

benzene is extended perpendicularly into a third dimension in a typical  $S_N2$ -type methyl-exchange configuration, while the entire complex remains connected to the active site by hydrogen bonds and the aluminum negative charge, allowing little to no room for flexibility. Deformation of an optimal  $S_N2$ -type geometry will invariably lead to an increased reaction barrier.<sup>[28]</sup>

Not surprisingly, the reaction barrier in the MFI topology (Figure 1c) is strongly dependent on the number of methyl substituents. For small polymethylbenzenes a steady decrease in both reaction barrier (from 145.5 to 79.1 kJ mol<sup>-1</sup>) and reaction energy (from 101.7 to 49.1 kJ mol<sup>-1</sup>) is observed.

From durene on, however, the transition state lacks sufficiently ample space to take on the optimal geometry, and the reaction barrier increases significantly to 90.9 kJ mol<sup>-1</sup>. However, the pentamethylbenzenium ion, which is not as bulky as the transition state, is more stable than the neutral species by 8.5 kJ mol<sup>-1</sup>. The geminal methylation of pseudocumene and pentamethylbenzene also has a low activation energy (79.1 and 81.3 kJ mol<sup>-1</sup>) and provides more reactive species for subsequent steps. Each additional methyl group imposes a constant conflict between two opposing effects: on the one hand it leads to a more reactive hydrocarbon-pool species as well as stronger electrostatic interaction with the framework, and on the other hand it is subject to the geometric constraints imposed by the zeolite topology. For HMB this combination of contradictory contributions leads to a reaction barrier of 126.2 kJ mol<sup>-1</sup> and reaction energy of 29.0 kJ mol<sup>-1</sup>, which is located between the values obtained for BEA and CHA. In a small-pore catalyst like HZSM-5, the formation of large cations is severely restricted, and the hydrocarbon pool will most likely consist of less sterically demanding methylated benzenes or might even be based on the methylation of smaller branched olefins rather than bulkier methylbenzenes.<sup>[29,30]</sup>

We conclude that specific combinations of organic reaction centers and the inorganic framework cooperate effectively in stabilizing intermediates and transition states that would, if considered separately, be of excessively high energy. These results offer additional support for the hydrocarbon-pool model by providing a first step towards alternative low-energy pathways for reactions that would otherwise have very high-energy intermediates, as, for example, in the direct oxonium ylide or carbene proposals.<sup>[5]</sup> Without the solvating effect of the zeolite framework, the number of methyl substitutions on the benzene ring can account for only a relatively minor decrease in both barrier height and reaction energy. The zeolite topology, however, plays a major role in reaction kinetics. For the geminal methylation of hexamethylbenzene the following order of reactivity according to topology is observed: CHA  $\gg$  MFI > BEA. The chabazite cages provide the perfect surroundings for a surprisingly stable heptamethylbenzenium cation, while the large beta cages favor neutral species over cations. In the MFI framework, on the other hand, transition-state-shape selectivity takes over for the bulkier methylbenzenes, and lesser methylated cations are the most likely intermediates. Immediately after submission of this paper, a communication by Svelle et al. was published online, including experimental confirmation of the higher activity of the lower methylbenzenes in H-ZSM5.<sup>[31]</sup>

Further theoretical insights into the effect of zeolite topology are desperately needed, if only to guide development of novel materials with a fine-tuned local spatial environment that optimizes catalytic activity, improves product selectivity, and simultaneously reduces coke formation. Additional insights might even be obtained from enzyme or homogeneous catalysis rather than from traditional zeolite chemistry.<sup>[32]</sup> To achieve these common goals, strong interaction between experimental work and computational modeling is indispensable.

## Experimental Section

All geometry optimizations were performed with the Gaussian03 package.<sup>[33]</sup> The 5T cluster, treated at the B3LYP/6-31g(d) level of theory,<sup>[34]</sup> was left unconstrained to verify the true nature of all stationary points. Zero-point-energy (ZPE) corrections were included. Starting from transition-state geometries, the quasi-IRC approach allowed the reactant and product geometries to be acquired. The calculations on the BEA, CHA, and MFI topologies were performed on 44T or 46T clusters at the ONIOM(B3LYP/6-31 + g(d):HF/6-31 + g(d))/ONIOM(B3LYP/6-31 + g(d):MND0) level of theory,<sup>[23,24]</sup> where the 5T zeolite active site as well as all organic species were considered at the high QM level. Only the saturating hydrogen atoms were fixed to prevent collapse of the cage. All other low-level framework atoms were allowed to fully adjust themselves to the large incorporated species. As elementary reaction steps were considered separately from adsorption/desorption requirements, only intrinsic energy barriers are shown in kJ mol<sup>-1</sup>.

Received: October 20, 2006

Published online: January 4, 2007

**Keywords:** ab initio calculations · arenes · heterogeneous catalysis · methanol-to-olefin process · zeolites

- 
- [1] M. Stocker, *Microporous Mesoporous Mater.* **1999**, *29*, 3–48.  
 [2] J. F. Haw, W. G. Song, D. M. Marcus, J. B. Nicholas, *Acc. Chem. Res.* **2003**, *36*, 317–326.  
 [3] W. G. Song, D. M. Marcus, H. Fu, J. O. Ehresmann, J. F. Haw, *J. Am. Chem. Soc.* **2002**, *124*, 3844–3845.  
 [4] D. M. Marcus, K. A. McLachlan, M. A. Wildman, J. O. Ehresmann, P. W. Kletnieks, J. F. Haw, *Angew. Chem.* **2006**, *118*, 3205–3208; *Angew. Chem. Int. Ed.* **2006**, *45*, 3133–3136.  
 [5] D. Lesthaeghe, V. Van Speybroeck, G. B. Marin, M. Waroquier, *Angew. Chem.* **2006**, *118*, 1746–1751; *Angew. Chem. Int. Ed.* **2006**, *45*, 1714–1719.  
 [6] P. W. Goguen, T. Xu, D. H. Barich, T. W. Skloss, W. G. Song, Z. K. Wang, J. B. Nicholas, J. F. Haw, *J. Am. Chem. Soc.* **1998**, *120*, 2650–2651.  
 [7] R. M. Dessau, *J. Catal.* **1986**, *99*, 111–116.  
 [8] I. M. Dahl, S. Kolboe, *J. Catal.* **1994**, *149*, 458–464.  
 [9] W. G. Song, J. F. Haw, J. B. Nicholas, C. S. Heneghan, *J. Am. Chem. Soc.* **2000**, *122*, 10726–10727.  
 [10] B. Arstad, S. Kolboe, *J. Am. Chem. Soc.* **2001**, *123*, 8137–8138.  
 [11] U. Olsbye, M. Bjorgen, S. Svelle, K.-P. Lillerud, S. Kolboe, *Catal. Today* **2005**, *106*, 108–111.  
 [12] T. Xu, D. H. Barich, P. W. Goguen, W. G. Song, Z. K. Wang, J. B. Nicholas, J. F. Haw, *J. Am. Chem. Soc.* **1998**, *120*, 4025–4026.  
 [13] J. F. Haw, J. B. Nicholas, W. G. Song, F. Deng, Z. K. Wang, T. Xu, C. S. Heneghan, *J. Am. Chem. Soc.* **2000**, *122*, 4763–4775.  
 [14] M. Bjorgen, F. Bonino, S. Kolboe, K.-P. Lillerud, A. Zecchina, S. Bordiga, *J. Am. Chem. Soc.* **2003**, *125*, 15863–15868.  
 [15] W. G. Song, J. B. Nicholas, A. Sassi, J. F. Haw, *Catal. Lett.* **2002**, *81*, 49–53.  
 [16] B. Arstad, J. B. Nicholas, J. F. Haw, *J. Am. Chem. Soc.* **2004**, *126*, 2991–3001.  
 [17] W. Song, H. Fu, J. F. Haw, *J. Am. Chem. Soc.* **2001**, *123*, 4749–4754.  
 [18] Z. M. Cui, Q. Liu, W. G. Song, L. J. Wan, *Angew. Chem.* **2006**, *118*, 6662–6665; *Angew. Chem. Int. Ed.* **2006**, *45*, 6512–6515.  
 [19] J. A. Martens, J. Perez-Pariente, E. Sastre, A. Corma, P. A. Jacobs, *Appl. Catal.* **1988**, *45*, 85–101.  
 [20] L. A. Clark, M. Sierka, J. Sauer, *J. Am. Chem. Soc.* **2004**, *126*, 936–947.  
 [21] A. M. Vos, X. Rozanska, R. A. Schoonheydt, R. A. van Santen, F. Hutschka, J. Hafner, *J. Am. Chem. Soc.* **2001**, *123*, 2799–2809.  
 [22] B. Arstad, S. Kolboe, O. Swang, *J. Phys. Chem. B* **2002**, *106*, 12722–12726.  
 [23] D. Lesthaeghe, V. Van Speybroeck, G. B. Marin, M. Waroquier, *Chem. Phys. Lett.* **2006**, *417*, 309–315.  
 [24] D. Lesthaeghe, G. Delcour, V. Van Speybroeck, G. B. Marin, M. Waroquier, *Microporous Mesoporous Mater.* **2006**, *96*, 350–356.  
 [25] D. S. Santilli, T. V. Harris, S. I. Zones, *Microporous Mater.* **1993**, *1*, 329–341.  
 [26] M. Schenk, S. Calero, T. L. M. Maesen, L. L. van Benthem, M. G. Verbeek, B. Smit, *Angew. Chem.* **2002**, *114*, 2609–2612; *Angew. Chem. Int. Ed.* **2002**, *41*, 2500–2502.  
 [27] A. Sassi, M. A. Wildman, H. J. Ahn, P. Prasad, J. B. Nicholas, J. F. Haw, *J. Phys. Chem. B* **2002**, *106*, 2294–2303.  
 [28] D. Lesthaeghe, V. Van Speybroeck, G. B. Marin, M. Waroquier, *J. Phys. Chem. B* **2005**, *109*, 7952–7960.  
 [29] H. Schulz, M. Wei, *Microporous Mesoporous Mater.* **1999**, *29*, 205–218.  
 [30] S. Svelle, B. Arstad, S. Kolboe, O. Swang, *J. Phys. Chem. B* **2003**, *107*, 9281–9289.  
 [31] S. Svelle, F. Joensen, J. Nerlov, U. Olsbye, K.-P. Lillerud, S. Kolboe, M. Bjorgen, *J. Am. Chem. Soc.* **2006**, *128*, 14770–14771.  
 [32] J. F. Haw, D. M. Marcus, *Top. Catal.* **2005**, *34*, 41–48.  
 [33] Gaussian03 (Revision B.03): M. J. Frisch et al., see the Supporting Information  
 [34] A. D. Becke, *J. Chem. Phys.* **1993**, *98*, 5648–5652.
-